

A New Morphodynamic Modelling Platform: Application to Characteristic Sandy systems of the Aquitanian Coast, France

N. Bruneau^{†‡}, P. Bonneton[‡], R. Pedreros[†], F. Dumas[∞] and D. Idier[†]

[†]Inland and Coastal Development Unit
BRGM
45060 Orléans Cedex 2
France

[‡]Department of Geology and Oceanography
UMR CNRS 5805 EPOC
University of Bordeaux I
33405 Talence Cedex
France

[∞]DYNECO/PHYSED Division.
IFREMER, BP 70
29280 Plouzané
France



ABSTRACT

BRUNEAU, N.; BONNETON, P.; PEDREROS, R.; DUMAS, F. and IDIER, D., 2007. A New Morphodynamic Modelling Platform: Application to Characteristic Sandy systems of the Aquitanian Coast, France. *Journal of Coastal Research*, SI 50 (Proceedings of the 9th International Coastal Symposium), 932 – 936. Gold Coast, Australia, ISSN 0749.0208

Along coasts, waves and wave-induced currents are the main factors of morphological evolution. A morphodynamic model is constructed to take into account tide changes, wind conditions and waves in the computation of the induced currents and morphological evolution. The spectral wave model SWAN, the shallow-water model MARS and a sedimentary module are coupled to create the morphodynamic model. First, we validate the hydrodynamics of the model on two characteristic complex bathymetries: an idealised subtidal crescentic bar and an intertidal ridge and runnel system. The crescentic bar induces wave energy focalisation zones which could give rise to transverse bars. Thus, we investigate the morphology evolution of the intertidal area. Simulations appear to show the formation of inner bars that connect the subtidal bar with the intertidal area.

ADDITIONAL INDEX WORDS: *Morphodynamic, Crescentic Bars, Ridges and Runnels, Aquitanian Coast, Modelling.*

INTRODUCTION

Nearshore areas are mainly studied in order to analyse morphodynamic evolution within a socio-economic and touristic framework. For security reasons, such as human safety and the protection of the natural environment and structures, we need to know currents, shoreline evolution and general erosion. Some research codes like Morpho50 (CABALLERIA *et al.*, 2002), Morpho55 (GARNIER *et al.*, 2006a), MORPHODYN (SAINT-CAST, 2002) and NearCoM (SHI, 2005) have proved their capacities to model wave-induced currents and morphological evolution. However, they do not take into account tide and meteorological phenomena. Thus, a new coupling has been made between the spectral wave model SWAN (BOUJ *et al.*, 2004), the shallow-water model MARS (PÉRENNE, 2005), well-tested for meteorological effects and tidal phenomena and a sedimentary module based on MORPHODYN (See Figure 1 for the global coupling scheme).

The model is initially implemented on idealised typical bars of the Aquitanian coast of France. This coast is composed of rhythmic complex sandbar systems like crescentic subtidal bars or ridge and runnel systems (LAFON *et al.*, 2004) which are interesting systems to validate the morphodynamic model. Some studies have already been focussed on hydrodynamics over these sandy systems (CASTELLE and BONNETON, 2003; CASTELLE and BONNETON, 2006a). Other studies have also shown the formation of crescentic bars (CASTELLE *et al.*, 2006b; GARNIER *et al.*, 2006b; SMIT *et al.*, 2005) starting from a disturbed bathymetry of a subtidal longshore regular bar and the generation of shore-oblique/transverse bars (GARNIER *et al.*, 2006a) but without taking into account tidal modulation in a continuous way.

First, this paper briefly describes the different modules of the morphodynamic model. Then we compare hydrodynamics with others studies and we analyse the impact of the crescentic bars on the intertidal morphodynamics.

METHODS AND MODELS

This section deals with the numerical models used for the coupling and equations solved by the models. SWAN and MARS are R&D codes but they are already used operationally taking into account real wind, pressure and tidal conditions (DUMAS *et al.*, 2006, www.previm.org).

The shallow-water model

The MARS model (Model for Applications at Regional Scale), developed at IFREMER, solves the unsteady shallow-water system of equations in two (depth-averaged) or three dimensions. We use for the present study the depth-averaged (2DH) model. MARS (PÉRENNE, 2005) is a finite-difference model designed to compute tide and wind-induced currents and it has been extensively tested on the whole French coast. Another considerable advantage is its rapid computational time due to the use of nested grids, which allows simulations from global to local scales. In the present work, a cartesian mesh is chosen since for the small size of the domains considered Coriolis and tide generated phenomena are negligible. Defining U_i as the component in the direction i of the depth-averaged current velocity, ζ as the free surface elevation and neglecting Coriolis, wind and tide effects, the governing equations, are in shortened formulation :

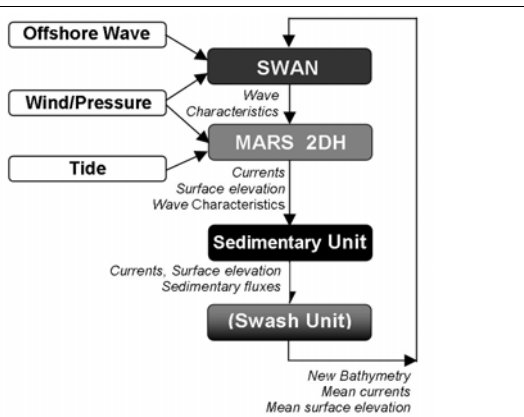


Figure 1. Global scheme of the morphodynamic model.

$$\frac{\partial \zeta}{\partial t} + \frac{\partial h U_i}{\partial x_i} = 0 \tag{1}$$

$$\frac{\partial U_i}{\partial t} + U_j \frac{\partial U_i}{\partial x_j} + g \frac{\partial \zeta}{\partial x_i} = \frac{\partial}{\partial x_j} \left(\nu_H \frac{\partial U_i}{\partial x_j} \right) - \frac{\tau_i^b}{\rho h} - \frac{1}{\rho h} \left(\frac{\partial S_{ij}}{\partial x_j} \right)$$

where g is gravity, ν_H is the horizontal eddy viscosity, ρ is the mass density of sea water, τ_i^b are the bed shear stress, h is the mean water depth and S_{ij} are the radiation stresses.

The spectral wave model

Wave characteristics are issued from SWAN (Simulating Waves Nearshore) third-generation numerical wave model. In this model, the evolution of the wave spectrum is described by the spectral action balance equation (BOOIJ et al., 2004). A Gaussian frequency spectrum is used as wave input. We applied a time-independent constant breaker parameter $\gamma = 0.73$ to model the energy dissipation due to depth-induced breaking (BATTJES and JANSEN, 1978). For the seabed friction model, we have chosen the formulation given by MADSEN et al. (1988) with an equivalent bed roughness length scale $K_N = 0.085m$ (CASTELLE et al., 2006).

The radiation stresses S_{ij} computed from the characteristics of the waves (significant wave height, mean wave direction, mean absolute wave period, etc.), are calculated with the following formulation coming from linear wave theory (DINGEMANS, 1997):

$$S_{ij} = \frac{E}{2} \left(\frac{k_i k_j}{k^2} \frac{2c_g}{c} + \delta_{ij} \left(\frac{2c_g}{c} - 1 \right) \right) \tag{2}$$

where E is the wave energy, c the wave velocity, c_g the group velocity and k the wave number.

A significant phenomenon in beach dynamics is the undertow. In order to model this current, a correction is added to the output velocities in the following way according to PHILLIPS (1977):

$$U_{i,Phillips} = U_i - \frac{Q_i^w}{h} \tag{3}$$

with $Q_i^w = Ek_i/(\rho ck)$, the volume flux associated with the organised wave motion.

To model the bottom shear stress induced by waves and currents, we implemented the weak flow approximation (LIU and DALRYMPLE, 1978):

$$\tau_i^b = \rho C_f U_w U_i \tag{4}$$

where U_w is the orbital velocity and C_f the bottom friction coefficient we take as constant and equal to 0.0048 according to CASTELLE et al. (2006).

The horizontal eddy viscosity can be written as the sum of a viscosity function of the latitude step (constant in our simulations) ν_0 and an eddy viscosity due to the turbulence generated by breaking waves in the surf zone applying the formulation of BATTJES (1975). Thus, we obtain the total viscosity ν_H :

$$\nu_H = \nu_0 + M h \left(\frac{D}{\rho} \right)^{1/3} \tag{5}$$

where D is the energy dissipation of the waves and M is a dimensionless coefficient. After sensitivity tests, M is chosen equal to 0.1 which is lower than fixed by CASTELLE et al. (2006) (who use 5) and which is the upper boundary of the interval (0.05 and 0.1) given in the Shorecirc user’s manual (SVENDSEN et al., 2004).

The sedimentary unit

An internal module was developed inside MARS to calculate the morphological evolution of the sandy seabed. This module is decomposed into two main parts: the computation of the transported sediment fluxes and the resolution of the sediment conservation law. In this first study, we do not take into account the swash zone.

The sediment fluxes

Following the development of the MORPHODYN model (SAINT-CAST, 2002), we implement the BAILLARD (1981) formulation which takes into account bed-load and suspension transport. Defining Q_b as the bed-load transport flux, $Q_{b\beta}$ as the component of bed-load transport by slope effect, Q_s as the suspension transport flux and its slope effect component by $Q_{s\beta}$, we obtain the transported sediment total flux Q_t :

$$\bar{Q}_t = \bar{Q}_b - \bar{Q}_{b\beta} + \bar{Q}_s - \bar{Q}_{s\beta} \tag{6}$$

with:

$$\bar{Q}_b = \frac{\varepsilon_c C_f}{g(s-1)\tan\varphi} \overline{\|U_b\|^2 \bar{U}_b}$$

$$\bar{Q}_{b\beta} = \frac{\varepsilon_c C_f}{g(s-1)\tan^2\varphi} \overline{\|U_b\|^3 \bar{\nabla} Z_b} \tag{7}$$

$$\bar{Q}_s = \frac{\varepsilon_s C_f}{g(s-1)\omega_s} \overline{\|U_b\|^3 \bar{U}_b}$$

$$\bar{Q}_{s\beta} = \frac{\varepsilon_s^2 C_f}{g(s-1)\omega_s^2} \overline{\|U_b\|^5 \bar{\nabla} Z_b}$$

where $\overline{\langle \cdot \rangle} = \frac{1}{T_m} \int_t^{t+T_m} \langle \cdot \rangle dt$, T_m is the mean wave period, ε_c and ε_s

are effectiveness factors, φ is the internal friction angle of the sediment equal to 32° (MIGNIOT, 1977), s relative density, ω_s the fall velocity of the suspended sediment, Z_b the bottom level and we made the approximation that the flow velocity close to the bottom U_b is given by:

$$\vec{U}_b(t) = \vec{U} + \vec{U}_w \cos(2\pi t/T_m) \quad (8)$$

where U_w is the orbital wave velocity. Asymmetric waves are not implemented in the present work.

The sediment conservation law

The new bottom level is computed solving the sediment conservation law with a simple centre second-order scheme. This equation can be written in the following way:

$$\frac{\partial Z_b}{\partial t} + \frac{1}{1-p} \bar{\nabla} \cdot \bar{Q}_i = 0 \quad (9)$$

where p is the sediment porosity.

The model bathymetries

The numerical ridge and runnel bathymetry and crescentic bathymetry have been created by CASTELLE (2004) from a synthesis of bathymetric surveys and SPOT images on the Aquitanian coast. The ridge and runnel bar (Figure 3) is built with a wavelength of 400 m which corresponds to the mean wavelength of this kind of system on the coast. A gentle uniform slope is used to extend the bar to the offshore boundary. The simulations are computed with a 10 m regular grid and periodic lateral boundary conditions. For the crescentic bar (Figure 4), the wavelength is equal to 1000 m, the offshore depth is 19 m at low tide to the shoreline and a uniform slope connects the intertidal domain with the subtidal bar. We use a uniform 20 m grid in both cross-shore and longshore directions with, in addition, periodic lateral conditions. To avoid problems due to lateral boundary conditions, SWAN computations are performed on a domain three times larger in the longshore direction.

Set-up modelling

In the depth-averaged current model MARS, the time step is a function of the Courant number. Here, the time step can vary between 5 and 20 s. For the complete coupling between SWAN, MARS and the sedimentary unit, a 1 hour time step is chosen to compute the new bottom level and the new characteristics of the waves. The tide is treated schematically and is representative of the Aquitanian Coast: a tidal range of 3 m, a tidal cycle of 12 h and a tide level evolving by 50 cm increments are used.

RESULTS

First, the numerical model is validated for two hydrodynamic cases: (1) a laboratory example, (2) characteristic bar systems presented previously: a subtidal crescentic bar and a ridge and runnel system. Then, results of the first morphological evolution on a couple of tidal cycles of the crescentic bar are shown.

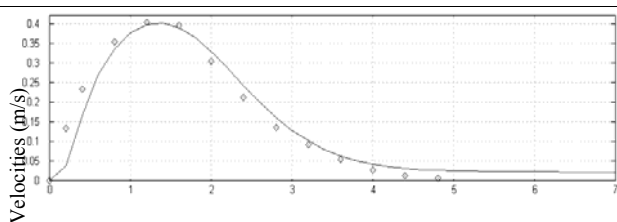


Figure 2. Comparison of the longshore velocities along a cross-shore profile between the model (plain line) and the measurements of VISSER, experiment 4 (points).

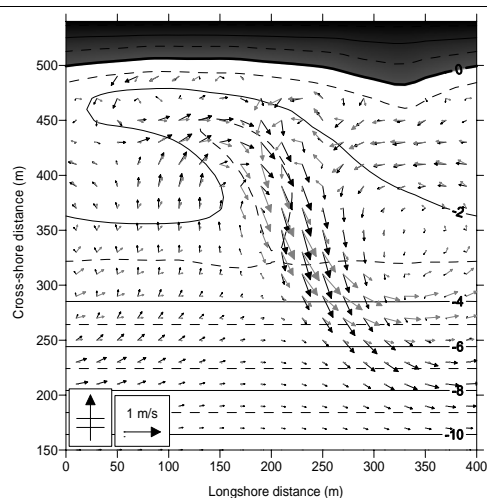


Figure 3. Wave-induced current vector map over the ridge and runnel system (bathymetry levels) at middle tide, $h_t = 2.96$ m. Wave conditions: $H_s = 1$ m, $T_m = 12$ s, $\theta = 0^\circ$. Black vectors represent the mean current without feedback of the currents on the waves and grey vectors with feedback.

Hydrodynamic validation

The comparison with the laboratory measurements of VISSER (1991) gives good results. Considering current feedback on waves (example on Figure 2), the correlation coefficient is $r^2 = 0.93$.

The two bar systems are more interesting examples to test the platform since they represent complex beach bathymetries where wave-induced currents are intense. Figure 3 shows the hydrodynamics over the ridge and runnel bar system at middle tide ($h_t = 2.96$ m over the level of reference). In order to compare the results with another study, the same wave conditions as CASTELLE and BONNETON (2006a) are used here: a 0° incident wave with a significant height $H_s = 1$ m and a mean wave period $T_m = 12$ s. Vector maps for two different radiation forcings are plotted on the Figure 3: the first (black vectors) represents the mean depth-averaged currents without the feedback of the hydrodynamics on the waves and the grey vectors with the feedback. With the wave/current interaction, the flows are channelled more intensely in the hollow of the runnel and are slightly greater (maximums are 0.87 m/s with feedback and 0.79 m/s without) and so is the induced impact on sedimentary transport. Comparison of the results with those of CASTELLE and BONNETON (2006a) are in agreement both for the form and the amplitude of the flows. The differences observed, close to the shoreline, can be explained because we have not taken into account the roller effect.

On Figure 4, the currents over the subtidal crescentic bar are represented for the following wave conditions: $H_s = 1.5$ m, $T_m = 12$ s and $\theta = 10^\circ$ at low tide. For the crescentic bar, simulation results are always close to CASTELLE (2004) but with some differences, maybe due to roller effects. Close to the shoreline, a longshore drift current is predominant with an average amplitude ranging between 0.2 and 0.4 m/s. The maximum intensity for the flows is found just behind the crescent crest where waves break and can reach up to 0.58 m/s at low tide. We already note that they are three significant rip currents that move during a tidal cycle and give rise to points of energy focalisation which can induce the formation of intertidal patterns.

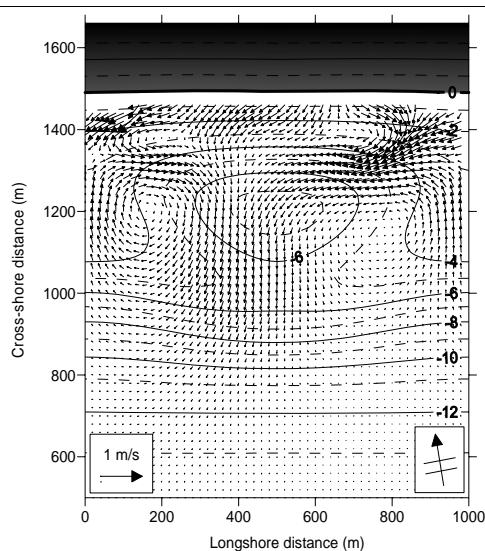


Figure 4. Wave-induced current vector map over the crescentic subtidal bar (bathymetry levels). The shoreline at low tide is 1 m over the reference level. Wave conditions: $H_s=1.5\text{m}$, $T_m=12\text{s}$, $\theta=10^\circ$.

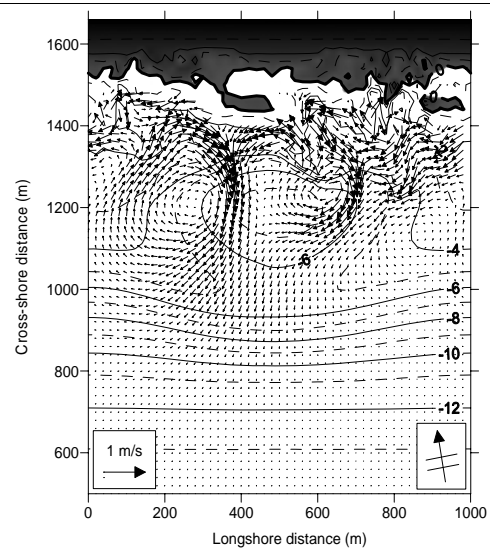


Figure 5. Wave-induced current vector map over the crescentic subtidal bar (bathymetry levels). $t = 36$ days. The shoreline at low tide is 1 m over the reference level. Wave conditions: $H_s=1.5\text{m}$, $T_m=12\text{s}$, $\theta=10^\circ$.

Morphological evolution

As we have explained previously, the crescent bar induces wave energy focalisation close to the shoreline. The tide level increases and decreases step by step allowing the breaking area and thus the energy focalisation zones, to move. Figure 5 shows, 36 days later, the new bathymetry and wave-induced currents again at low tide and for the same wave conditions, which remain identical during the simulation. Two intertidal patterns are observed: their bathymetries correspond to areas where there are energy focalisations. The new forms channel the currents and the depth-averaged currents are stronger than the initial flows (Figure 4). In order to distinguish in detail the morphological evolution, the difference between the 36-days bathymetry and initial bathymetry are shown in Figure 6. We observe generation of two rhythmic runnels with a wavelength of about 450 m, which is the same order as the mean width of ridge and runnel systems on the Aquitanian coast and corresponds to the area where rip currents are significant. Inner bars have been generated with crescent patterns that link the ridge and connect the subtidal and the intertidal systems. The inner bar is not always visible on the Aquitanian coast but it can sometimes be observed (Figure 7).

DISCUSSION

The results for complex bathymetries are consistent with previous studies. In order to completely validate the hydrodynamics, the model will be tested on complex real beaches. CASTELLE and BONNETON (2003) showed that the wave refraction over a crescentic bar generates energy focalisation areas and thus they conjecture that it can promote the formation of intertidal patterns as ridge and runnel. The results shown here support this view. However, the runnels created by the morphodynamic model are lengthened in up-current direction whereas some down-current systems are also observed along the Aquitanian coast. The direction of the sandy forms can come from the computation of sedimentary fluxes. Indeed, a recent study (GARNIER *et al.*, 2006a) shows the influence of the sediment formulation parameterisation on the direction of oblique/transverse bars. This would tend to

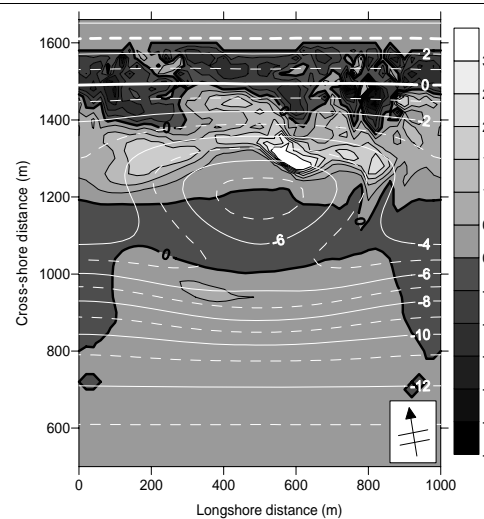


Figure 6. Difference (m) between the bathymetry at $t = 36$ days and the initial bathymetry of the crescentic bar superposed with the initial bathymetry levels. Dark colors mean erosion and light colors accretion. Thick white lines represent the limits of initial intertidal zone.

demonstrate the unstable character of the intertidal patterns unlike for subtidal bars. Different sediment formulations – Bailard (CASTELLE *et al.*, 2006b), Bijker (SMIT *et al.*, 2005), general total load sediment flux (GARNIER *et al.*, 2006b) – have shown the formation of crescentic subtidal bars that seem to be a stable pattern of the subtidal domain. To go further it would be necessary to conduct some sensitivity tests with different initial bathymetries, various sediment formulations and parameterisations. This model has also generated inner crescent bars that have been previously observed by CASTELLE (2004) or SMIT *et al.* (2005) (see Figure 7).

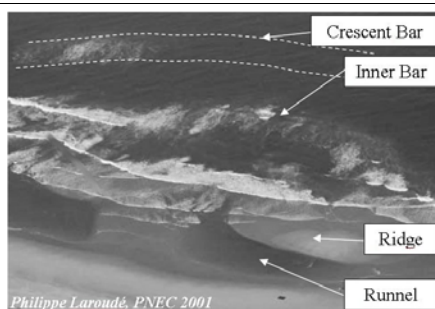


Figure 7. Inner bar on the Truc Vert beach during PNEC 2001.

Moreover, in the different tests we discussed above, various physical phenomena can explain the observed morphological patterns. Now we have to investigate the importance of other phenomena such as asymmetrical waves or roller effects that have a significant impact on the hydrodynamics (GODA, 2006) and on the morphodynamics. These are not taking into account in the present study. In addition, it is planned to input real tide since it causes regular erosion of the intertidal domain and current feedback.

CONCLUSION

In the present paper, a morphodynamic model, based on the SWAN and MARS models has been presented. It reproduces quite well wave-induced currents over complex idealised bar systems. The importance of crescentic bars on the circulation cells and energy focalisation areas has also been shown. Rip currents induced by wave refraction over the crescent could be at the origin of some intertidal systems connected with the subtidal bar by an inner bar. Further investigations are needed in order to validate the whole morphological model for a real beach.

ACKNOWLEDGEMENTS

The present work is carried out within the framework of a project between UMR EPOC University Department, BRGM and IFREMER R&D. The authors would like to thank Bruno Castelle for his contribution and John Douglas for reviewing the English.

LITERATURE CITED

- BAILLARD, J.A., 1981. An Energetic Total Load Sediment Transport Model For a Plane Sloping Beach. *Journal of Geophysical Research*, 86(C11), 10938-10954.
- BATTJES, J., 1975. Modelling of turbulence in the surf zone. *Symposium on Modelling Techniques* (San Francisco, United States, ASCE), pp. 1050-1061.
- BATTJES, J. and JANSSEN, J., 1978. Energy loss and set-up due to breaking of random waves. *Proceedings of the 16th International Conference on Coastal Engineering* (Hamburg, Germany, ASCE), pp. 569-587.
- BOOIJ, N.; HAAGSMA, I.J.G.; HOLTHUIJSEN L.H.; KIEFTENBURG, A.T.M.M.; RIS, R.C.; VAN DER WESTHUYSEN A.J. and ZIJLEMA M., 2004. *Swan Cycle III version 40.41*. User's Manual, 115p.
- CABALLERIA, M.; COCO, G.; FALQUES, A.; HUNTLEY D.A., 2002. Self-organisation mechanisms for the formation of nearshore crescentic and transverse sand bars. *Journal of Fluid Mechanics*, 465, 379-410.
- CASTELLE, B. and BONNETON, P., 2006a. Modélisation du courant sagittal induit par les vagues au-dessus des systèmes barre/baïne de la côte aquitaine (France). *Geoscience*, 338, 711-717.
- CASTELLE, B.; BONNETON, P. and BUTEL, R., 2006b. Modélisation du festonnage des barres sableuses d'avant-côte : application à la côte Aquitaine, France. *Geoscience*, 338, 795-801.
- CASTELLE, B.; BONNETON, P.; SÉNÉCHAL, N.; DUPUIS, H.; BUTEL, R. and MICHEL, D., 2006c. Dynamics of wave-induced currents over an alongshore non-uniform multiple-barred sandy beach on the Aquitanian coast, France. *Continental Shelf Research*, 26, 113-131.
- CASTELLE, B., 2004. Modélisation de l'hydrodynamique sédimentaire au-dessus des barres sableuses soumises à l'action de la houle : application à la côte Aquitaine. Bordeaux, France: University of Bordeaux I, Ph.D. thesis, 344p.
- CASTELLE, B. and BONNETON, P., 2003. Nearshore waves and currents over crescentic bars. *Journal of Coastal Research, SI 39 (Proceedings of the 8th International Coastal Symposium)* (Itajai, Brazil), pp.
- DINGEMANS, M., 1997. *Water Wave Propagation Over Uneven Bottoms*. Advanced Series on Ocean Engineering 13, 1016p.
- DUMAS, F.; COAT, A.; FRELIN, C.; GIRARD, F.; LECORNU, F.; LE ROUX, J.F. and SEILLE, B., 2006. An operational demonstrator of oceanographic interest over the Iroise Sea. *Proceedings of the Operational Coastal Oceanography* (Brest, France).
- GARNIER, R.; CALVETE, D.; FALQUES, A. and CABALLERIA, M., 2006a. Generation and nonlinear evolution of shore-oblique/transverse sand bars. *Journal of Fluid Mechanics*, 527, 327-360.
- GARNIER, R.; BONNETON, P.; FALQUES, A. and CALVETE, D., 2006b. Modélisation de la formation et de l'évolution non linéaire des barres en croissants de la côte Aquitaine. *IXème Journée Nationales Génie Côtier-Génie Civil* (Brest, France).
- GODA, Y., 2006. Examination of the influence of several factors on longshore current computation with random waves. *Coastal Engineering*, 53, 157-170.
- LAFON, V.; DE MELO APOLUCENO, D.; DUPUIS H.; MICHEL D.; HOWA H. and FROIDEFOND J.M., 2004. Morphodynamics of nearshore rhythmic sandbars in a mixed-energy environment (SW France): I. Mapping beach changes using visible satellite imagery. *Estuarine, Coastal and Shelf Science*, 61, 289-299.
- LIU, P. and DALRYMPLE, R., 1978. Bottom frictional stresses and longshore currents due to waves with large angle of incidence. *Journal of Marine Research*, 36, 357-375.
- MIGNIOT, C., 1977. Action des courants, de la houle et du vent sur les sédiments. *La Houille Blanche*, 1, 9-47.
- PÉRENNE, N., 2005. *MARS a Model for Applications at Regional Scale, Documentation scientifique version 1.0*. User Manual, 45p.
- PHILLIPS, O., 1977. *The dynamics of the upper ocean*. Cambridge : Cambridge University Press.
- SAINT-CAST, F., 2002. Modélisation de la morphodynamique des corps sableux en milieu littoral. Bordeaux, France: University of Bordeaux I, Ph.D. thesis, 247p.
- SHI, F.; KIRBY, J.T.; NEWBERGER, P. and HAAS, K., 2005. *NearCoM Master Program, Version 2005.4*: User's manual and module integration, 91p.
- SMIT, M.W.J.; RENIERS, A.J.H.M.; STIVE, M.J.F., 2005. Nearshore bar response to time varying conditions. *Proceedings of the 5th International Conference on Coastal Dynamics* (Barcelona, Spain).
- SVENDSEN, I.A.; HAAS, K. and ZHAO, K., 2004. *Quasi-3D nearshore circulation model Shorecirc version 2.0*. User's Manual, 65p.
- VISSER, P.J., 1991. Laboratory measurements of uniform longshore currents. *Coastal Engineering*, 15, 563-593.